Electronic Supplementary Material (ESI) for ChemComm.

ELECTRONIC SUPPLEMENTARY INFORMATION

On-surface self-organization of a robust metal–organic cluster based on copper(I) with chloride and organosulphur ligands

G. Otero-Irurueta, I. Hernández, J. I. Martínez, R. Percy-Palacios, J. Palomares, M. F. López, A. I. Gallego, S. Delgado, F. Zamora,* J. Mendez, and J. A. Martin-Gago*

Experimental Section

1. Synthesis and characterization of $[Cu_4(\mu_3\text{-}Cl)_4(\mu\text{-}pymS_2)_4]$

All chemicals were of reagent grade and were used as commercially obtained. The dipyrimidinedisulfide (pym_2S_2) ligand was prepared according to the published procedure [S1]. The reactions were carried out under a dry argon atmosphere using Schlenk techniques and vacuum-lines systems. FTIR spectra (KBr pellets) were recorded on a Perkin-Elmer 1650 spectrophotometer. Elemental analyses were performed by the Microanalysis Service of the Universidad Autónoma de Madrid on a Perkin-Elemer 240 B microanalyzer.

A solution of $CuCl_2{\cdot}2H_2O$ (0.048 g, 0.28 mmol) in 6 mL of ethanol was slowly dropped on a solution of pym_2S_2 (0.062 g, 0.28 mmol) in 8 mL ethanol:CH_3CN (1:1). After 3 weeks, yellow crystals of $[Cu_4(\mu_3\text{-}Cl)_4(\mu\text{-}pymS_2)_4]$ were obtained upon slow concentration. The crystals were separated by hand, washed with diethylether and dried on air. Yield (0.040 g, 44 %). Anal. Caldc. (%) for $C_8H_6ClCuN_4S_2$: C, 29.89; H, 1.87; N, 17.43; S, 19.92; Found C, 29.37; H, 2.07; N, 17.02; S, 19.4%. IR (KBr, cm^{-1}): 1577(s), 1552(vs), 1388(vs), 1377(vs), 1168(s), 807(m), 771(m), 758(m), 743(m).

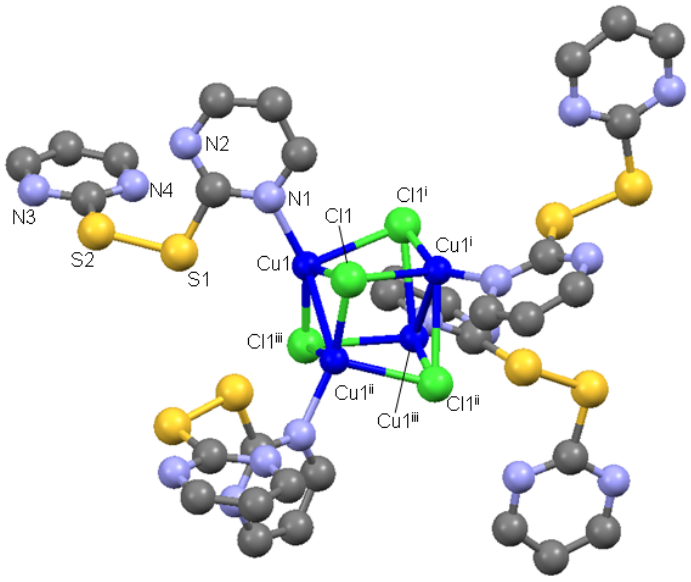

Figure S1. Ball-and-stick model of the $Cu^{I}_4(\mu_3\text{-}Cl)_4$ $(\mu\text{-}pymS_2)_4$ molecule used in this work. Cu atoms are in blue, Cl in green, C in black, N in light blue, S in yellow and H in white (representation from X-ray structural data reference 13 of manuscript)

2. On-surface experimental details

Experiments were carried out in an Ultra High Vacuum (UHV) chamber with base pressure of $1x10^{-10}$ mbar. The Cu(110) was cleaned by the conventional procedure of repeated cycles of argon sputtering and annealing at 800K. After preparation the sample surface was checked by STM and LEED prior to the molecular deposition.

The molecules were introduced into a homemade evaporator source consisting in a tantalum envelope with two rods and a fixed thermocouple. For heating up it an electrical current is directly flowed through the envelope allowing a high level of temperature control. In order to avoid any residual contamination in the molecular powder we degassed the molecules during hours at 350 K in an independent vacuum chamber. The molecular depositions were carried out by introducing the evaporator source in front of the clean Cu(110). The minimum sublimation temperature that we experimentally found was 370 K. Under these conditions the necessary time for fully cover the sample is 60 minutes. The aim of our experimental recipe is to maximize the structural ordering during the molecular deposition.

STM images were acquired at room temperature with a commercial Scanning Tunneling Microscope (VT-STM-XA, Omicron Nano Technology GmbH) in constant current mode [S2]. The voltages of polarization that we are given hereafter are applied on the tip maintaining the Cu(110) at ground. For data acquisition and analysis we used the WSxM software [S3].

3. Evolution with the coverage

In order to deeply characterize the molecular growth and the formation of the (3x5) superstructure we followed the molecular deposition with STM and LEED. Figure S2 shows a series of STM images obtained after depositing 0.1 ML (a), 0.5 ML (b), 0.75 ML (c) and 1 ML (d). At this particular conditions, the molecular structure are imaged darker than the Cu substrate. Even in the case of low coverages (a) the molecules self-organize forming the characteristics chains. We note that the step edges of the Cu(110) surface are preferential absorption sites for the molecular growth (brown arrows indicated in Figure S2a). As the coverage is increased the chains grow, invading the terraces in both main crystallographic directions (Figure S2b). Increasing the molecular coverage (Figure S2c-d) the structure cover completely the Cu(110) surface.

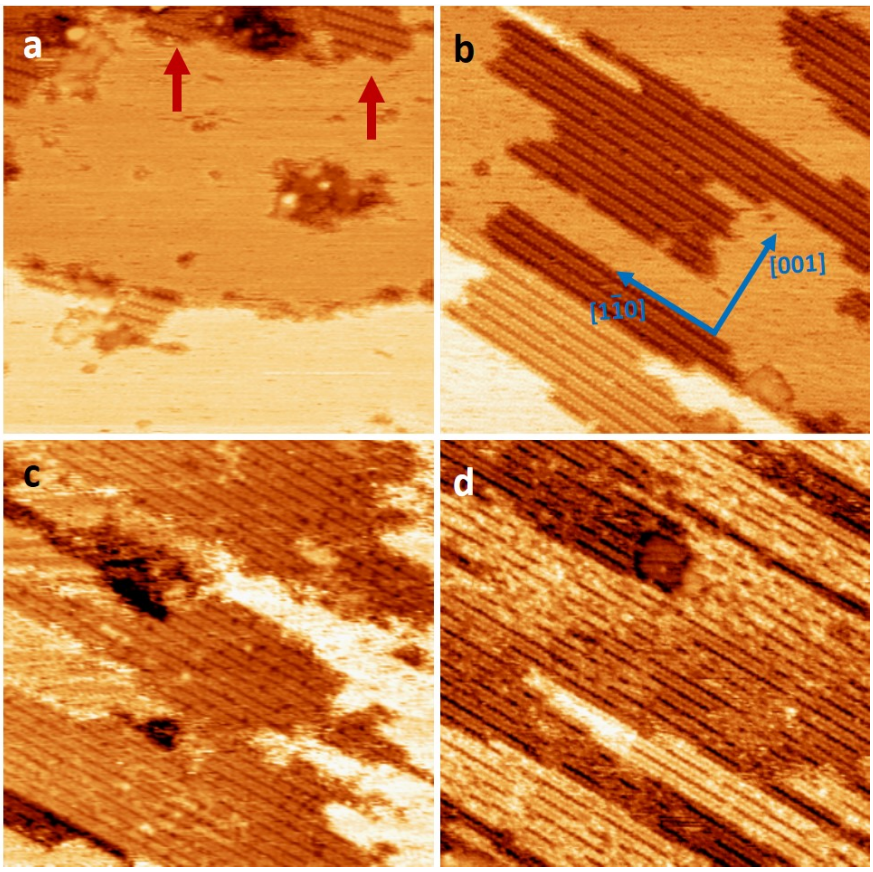

Figure S2. STM images as the coverage is increased. a) 0.1 ML, the step edges of the Cu(110) surface are preferential adsorption sites for low coverages (brown arrows). b) 0.5 ML, c) 0.75 ML and d) 1 ML the chains grow step by step invading the whole surface.

Figure S3 shows the LEED patterns obtained for clean Cu(110) surface (a) and after depositing 0.5 ML of molecules (b). In the clean surface case the expected rectangular pattern is observed while after the molecular deposition new extra spots were detected corresponding to a (3x5) superstructure.

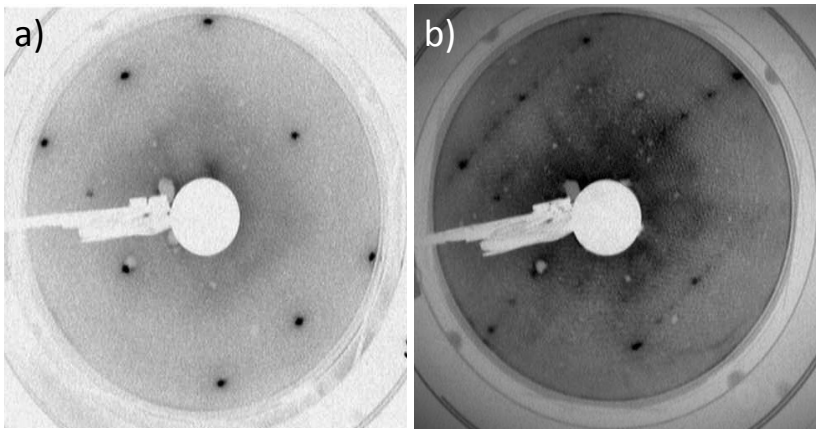

Figure S3. LEED pattern at an energy of 65 eV for the clean surface of the Cu(110) (a) and after depositing 0.5 ML of $Cu^{I}_{4}(\mu_3\text{-}Cl)_4$ $(\mu\text{-}pymS_2)_4$ molecules, at an energy of 95 eV (b). The molecules self-organize forming a (3x5) superstructure.

4. Evolution with time

Successive STM images of the same area showing that at intermediate coverage the molecules diffuse on the surface at room temperature. Figure S4 shows a series of four consecutive STM images recording during 20 minutes. Notice the region marked with the black arrow is changing during the sequence. In particular, molecules at the end of the chains desorb from the molecular structure, diffuse on copper surface and reattach at a new chain.

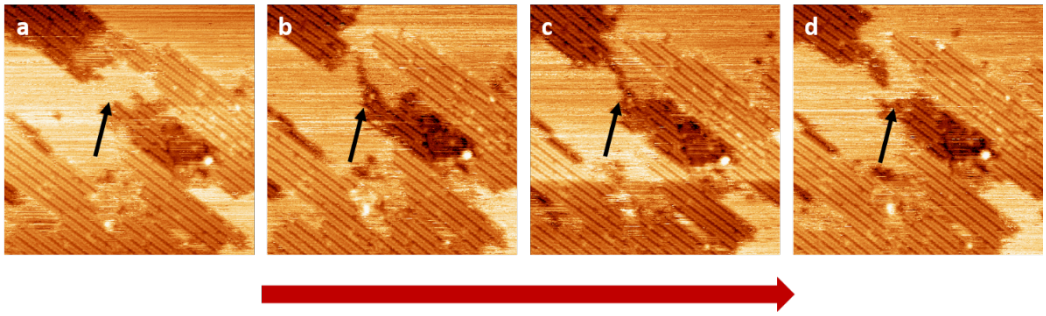

Figure S4. Four STM images acquired at the same region with increasing time. The time difference between images is 5 minutes (Total time: 20min). Black arrows indicate changes at the edge of the chains. Tunnel parameters: a-d) (50x50)nm^2, I=0.033nA, V=1250mV

5. XPS analysis

X-ray photoelectron spectroscopy (XPS) was used to characterize the chemical composition of the sample. The XPS measurements were performed in an independent UHV system with a base pressure of 10^{-9} mbar using a hemispherical electron energy analyzer (SPECS Phoibos 150 spectrometer) and a monochromatic AlKα (1486.74 eV) X-ray source. The spectra were recorded at normal emission take-off angle using an energy step of 0.1 eV and a pass-energy of 20 eV, which provides an overall instrumental peak broadening of 0.55 eV [S4]. All binding energies were referenced to the C1s peak (284.6 eV).

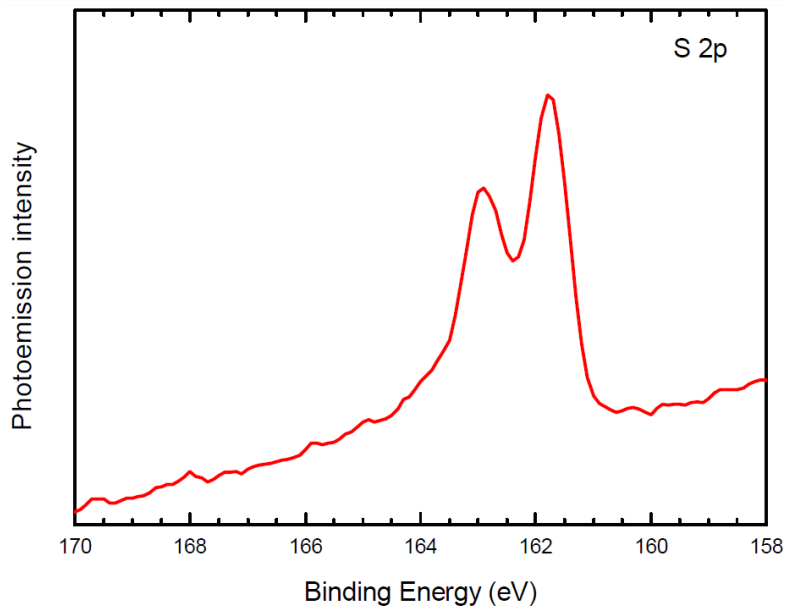

Figure S5. Monochromatic XPS high resolution spectrum of S 2p of Cu_4Cl_4 metal-organic cluster deposited on Cu(110) surface.

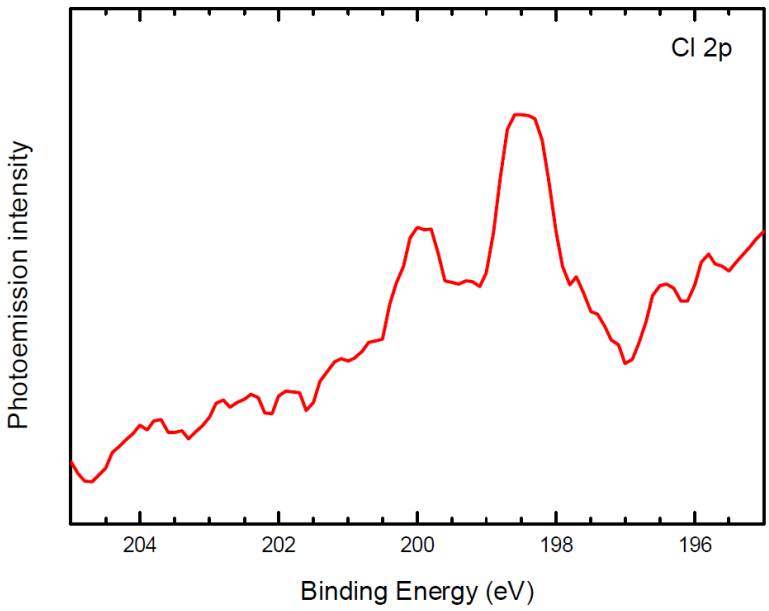

Figure S6. Monochromatic XPS high resolution spectra of Cl 2p of Cu_4Cl_4 metal-organic cluster deposited on Cu(110) surface.

6. Theoretical results

6.1. Computational details

For the ab-initio atomistic and molecular dynamics simulations of the proposed model analyzed in this study, Density Functional Theory (DFT) was used effectively combining the localized-basis-set and plane-wave schemes as implemented in the FIREBALL [S5] and PWSCF [S6] simulation packages, respectively. A perturbative van der Waals (vdW) correction was used to check the reliability of the adsorbed adlayer configuration. For this purpose, we have used an empirical efficient vdW R^{-6} correction to add dispersive forces to conventional density functional (DFT+D) [S7]. Within this approach, the vdW correction is added to the DFT total energy by the expression:

$$E_{vdW} = \sum_{i,j} \frac{C_{ij}}{R_{ij}^6} f(R_{ij}), \qquad \text{(eq. 1)}$$

where C_{ij} and R_{ij} are the vdW coefficients and the distance between atom i and j, respectively. The vdW coefficients can be calculated as described by Elstner et al. [S8]. In eq. (1), $f(R_{ij})$ is a damping function that prevents a divergence in the energy as R_{ij} tends to zero as:

$$f(R_{ij}) = \left(1 - \exp\left[-3.0\left(\frac{R_{ij}}{R_{0ij}}\right)^7\right]\right)^4, \qquad \text{(eq. 2)}$$

where R_{0ij} is the sum of atomic van der Waals radii. They can be calculated from the vdW radii provided by Gavezzotti and co-workers [S9] – see further details on this approach in Refs. [S7, S8] and references therein –. The exchange-correlation (XC) effects have been accounted by using the local density PW91 parametrization[S9] and norm-conserving scalar-relativistic pseudopotentials[S10] have been considered to model the ion-electron interaction. For the localized-basis-set code FIREBALL, a $sp^3d^5d^{*5}$ basis set of single and double numerical atomic

orbitals (one s, three p, and a double set of five d orbitals) was employed for Cu, a double numerical $sp^3s^*p^{*3}$ basis set for H, and optimal polarized sp^3d^5 basis sets for C, N, S, Cl. For the plane-wave code PWSCF, a plane-wave basis set with kinetic energy cutoff as high as 30 Ry was used. In the calculations the Brillouin zone (BZ) was sampled by means of a [4×4×1] Monkhorst-Pack grid [S11] guaranteeing a full convergence in energy and electronic density. The Cu(110) surface was modelled in a repeated slab geometry: i) a slab of four Cu(110) layers with a minimum distance of ≈ 25 Å of vacuum between neighboring cells along the axis perpendicular to the surface, large enough to minimize any possible inter-molecular interaction between neighboring cells.; as well as ii) full periodic boundary conditions representing an infinite Cu(110) surface. Each substrate physical layer contained 48 Cu atoms, and the size of the unit cell in the direction parallel to the surface was (18.1 × 15.3) $Å^2$. To define the equilibrium properties of the structural configuration we carried out a full dynamical-quenching geometry optimization, and only the two bottom Cu(110) physical layers were kept fixed. Two additional Cu(110) layers were accounted for the calculations of the energetics, electronic structure, and theoretical STM imaging.

6.2. Theoretical STM imaging

In our STM approach, tunneling currents for the STM images have been calculated using a Keldysh–Green function formalism, together with the first-principles tight-binding Hamiltonian obtained from the local-orbital DFT-FIREBALL method (as explained in detail elsewhere [S5,S12,S13]). Some examples of the application of this approach can be found in references [S14-S16]; in particular, reference [S14] is an excellent example of how the accurate theoretical simulation of STM images, and its comparison with high-quality experimental UHV-STM images, can guide us towards the correct atomic structure of an organic molecule on a metal substrate. In order to obtain accurate STM images and tunneling currents, to be compared with our experimental UHV-STM images, we used an efficient STM theoretical simulation technique that includes – by construction – a detailed description of the electronic properties of both the tip and the sample. Using this technique, based on an effective combination of a Keldysh Green's function formalism and local orbital density functional theory [S12, S13], we split the system into sample and tip, where the sample here is the proposed interfacial model. In these calculations we have assumed to simulate the scanning with a W-tip formed by 5 protruding atoms (one of them in the apex) attached to an extended W(100)-crystal. Within this approach, in the tunneling regime at low temperature, the STM current is given by [S12, S13]:

$$I = \frac{4\pi e^2}{\hbar}\int_{E_F}^{E_F+eV_s} d\omega Tr[T_{ts}\rho_{ss}(\omega)T_{st}\rho_{tt}(\omega - eV)], \qquad \text{(eq. 3)}$$

where V_s is the surface voltage, ρ_{tt} and ρ_{ss} are the density of states (DOS) matrices – in the local orbital basis – associated with the tip and sample, whilst T_{ts} and T_{st} are the local orbital Hamiltonian matrices coupling tip and simple (see Refs. [S12, S13] for details). Thus, the overlapping Hamiltonian is obtained by using a dimer approximation: a dimer formed by one W atom (corresponding to the tip) and another one (H, C, N, S, Cl and Cu coming from the sample) is calculated for different atom–atom distances and for all the non-zero interactions, using the Keldish-Green formalism to propagate the tunnel current between both subsystems. The theoretical STM images have been obtained at constant-current scanning conditions, moving the W-tip perpendicularly to the sample in each scanning stage to search a pre-selected fix value of the tunnel current. The theoretical scanning parameters used here were Itunnel = 0.5 nA, with $V_{substrate}$ varying up to +2 V above the Fermi energy, in order to mimic the experimental procedure.

6.3 Geometrical model and energetic considerations

Despite of its evident structural complexity, in order to construct a realistic interfacial model of the ensambling of these molecules on the Cu(110) substrate to carry out the theoretical calculations, we have made use of all the available experimental STM information shown in this study. Important information extracted from the experimental STM images includes the molecule on-surface orientation, as well as the most representative measurable inter/intra-molecular distances, which have been used as a crucial guidance to construct the starting geometry. On that basis, the only geometrical model fitting the main features observed in the UHV-STM images is that one shown in Fig. 2, where the molecular packing is deeply explained in detail in the main text. The only free-parameter to be elucidated by theoretical considerations is, given the fix molecule on-surface orientation and the proposed molecular packing model, the optimal search of the most stable on-surface adsorption site. For that purpose, we have performed structural optimization calculations of the molecule on Cu(110) on four inequivalent adsorption on-surface positions: with the center of mass of each molecule lying "ontop" a Cu atom, on a short Cu-Cu bridge, on a long Cu-Cu bridge and on a "hollow". The results obtained from the dynamical quenching relaxation processes reveal very similar adsorption energies for the four different cases analyzed, ranging between 1.45 and 1.65 eV per molecule. The ground-state configuration of the system, yielding an adsorption energy of 1.65 eV/molecule, corresponds to the molecule lying "ontop" a Cu atom at a distance of 1.36 Å above the topmost Cu surface layer. At this point it is important to emphasize the important role played by the vdW forces in the molecular adsorption distances and energies for this interface. The above-mentioned vdW-DFT framework (DFT-D) [S7] leads to a significant increase of the adsorption energies and distances of around 20% and 15%, respectively, w.r.t. a conventional DFT framework.

On the other hand, as mentioned in the main text, the same molecular arrangement experimentally detected on Cu(110) may form *a priori* on the Cu(111) surface, given the commensuration equivalence between different surfaces of *fcc* crystals (case of Cu). In order to theoretically check the influence of the particular Cu surface on the molecular distances, energetics, and STM-imaging, we have analysed this case within the same theoretical framework. The Cu(111) surface was modelled in a repeated slab geometry: i) a slab of four Cu(111) layers with a minimum distance of ≈ 25 Å of vacuum between neighboring cells along the axis perpendicular to the surface, large enough to minimize any possible inter-molecular interaction between neighboring cells.; as well as ii) full periodic boundary conditions representing an infinite Cu(111) surface. Each substrate physical layer contained 48 Cu atoms, and the size of the unit cell in the direction parallel to the surface was (18.1 × 15.3) $Å^2$. To define the equilibrium properties of the structural configuration we carried out a full dynamical-quenching geometry optimization, and only the two bottom Cu(111) physical layers were kept fixed. Two additional Cu(111) layers were accounted for the calculations of the energetics, electronic structure, and theoretical STM imaging.

The results of the calculations reveal no significant variations neither in distances, adsorption energies or STM image morphology between both analyses on Cu(110) and Cu(111). In particular, four inequivalent adsorption sites have been analysed in this case, yielding adsorption energies ranging between 1.34 and 1.52 eV/molecule. For the Cu(111) surface, the ground-state configuration of the system, yielding an adsorption energy of 1.52 eV/molecule, corresponds, once again, to the molecule lying "ontop" a Cu atom at a distance of 1.50 Å above the topmost Cu surface layer (to be compared with the 1.65 eV/molecule, and the 1.36 Å for the case of the Cu(110) surface). Besides, regarding the calculated STM image for the Cu(111), and similarly to the Cu(110) case, the distance between two consecutive dark stripes is 1.8 nm along the [1-21] crystallographic direction, while the distance between two consecutive bumps is 0.76 nm along the [-101] direction for this surface, just the same

distances obtained for Cu(110). This similar behaviour on two essentially different Cu surfaces gives idea about the robustness of the intermolecular packing.

References

[S1] R.Leino, J. E. Lonnqvist, *Tetrahedron Lett.* **2004**, *45*, 8489.
[S2] Omicron Nanotechnology, VT STM XA, *User´s Guide* 2005, Version 1.0.
[S3] I. Horcas et al. *Rev. Sci. Instrument.* 2007, **78**, 013705.
[S4] G. Otero *et al.*, *Nature* 2008, **454**, 865.
[S5] J. P. Lewis, *et al.Phys. Status Solidi B* 2011, **248**, 1989.
[S6] P. Giannozzi, S. *et al.J. Phys.: Condens. Matter.* 2009, **21**, 395502.
[S7] S. Grimme, *J. Comp. Chem.* 2006, **27**, 1787.
[S8] V. Barone, *et al.J. Comput. Chem.*2009, **30**, 934.
[S9] J. P. Perdew, *et al.*, *Phys. Rev. B* 1992, **46**, 6671.
[S10] D. Vanderbilt, *Phys. Rev. B*.1990,**41,**7892.
[S11] D. J. Chadi, and M. L. Cohen, *Phys. Rev. B 1973,* **8**, 5747.
[S12] J. M. Blanco, *et al.*, *Phys. Rev. B* 2004, **70**, 085405.
[S13] J. M. Blanco, F. Flores, and R. Pérez, *Prog. Surf. Sci.* 2006, **81**, 403.
[S14] J. I. Martínez, *et al.*, *Phys. Rev. Lett.* 2012, **108**, 246102.
[S15] J. I. Martínez, *et al.*, *Phys. Stat. Sol. B* 2011, **248**, 2044.
[S16] E. Abad, *et al.*, *J. Chem. Phys.* 2011, **134**, 044701.